β-Carotene Redox Reactions in Photosystem II: Electron Transfer Pathway†

Peter Faller,*,‡ Andy Pascal,§,|| and A. William Rutherford‡

Section de Bioénergétiques and Section de Biophysique des Protéines et des Membranes, CEA CNRS URA 2096, CE Saclay 91191 Gif-sur-Yvette Cedex, France, and Facolta di Scienze MM.FF.NN. Biotechnologie Vegetali, Universita di Verona, Strada le Grazie, 37134 Verona, Italy

Received November 10, 2000

ABSTRACT: A carotenoid (Car), a chlorophyll (Chl_Z), and cytochrome b_{559} (Cyt b_{559}) are able to donate electrons with a low quantum yield to the photooxidized chlorophyll, $P680^+$, when photosystem II (PSII) is illuminated at low temperatures. Three pathways for electron transfer from Cyt b_{559} to $P680^+$ are considered: (a) the "linear pathway" in which Cyt b_{559} donates via Chl_Z to Car, (b) the "branched pathway" in which Cyt b_{559} donates via Car and where Chl_Z is also able to donate to Car, and (c) the "parallel pathway" where Cyt b_{559} donates to P680 without intermediate electron carriers and electron donation from Chl_Z and Car occurs by a competing pathway. Experiments were performed using EPR and spectrophotometry in an attempt to distinguish among these pathways, and the following observations were made. (1) Using PSII with an intact Mn cluster in which Cyt b_{559} was preoxidized, Car oxidation was dominant upon illumination at $\leq$20 K, while electron donation from Chl dominated at $>$120 K. (2) When Cyt b_{559} was prereduced, its light-induced oxidation occurred at $\leq$20 K in what appeared to be all of the centers and without the formation of a detectable Car^+ intermediate. The small and variable quantity of Car^+ photoinduced in these experiments can be attributed to the residual centers in which Cyt b_{559} remained oxidized prior to illumination. (3) The relative rates for irreversible electron donation from Cyt b_{559} and Car were determined indirectly at 20 K by monitoring the flash-induced loss of charge separation (i.e., the accumulation of Cyt $b_{559}{}^+Q_A{}^-$ or $Car^+Q_A{}^-$). Similar yields per flash were observed (13% for Cyt b_{559} and 8% for Car), indicating similar donation rates. The slightly lower yield with Car as a donor is attributed at least in part to slow charge recombination occurring from the $Car^+Q_A{}^-$ radical pair in a fraction of centers. (4) Light-induced oxidation of Cyt b_{559} and Car at 20 K was monitored directly by EPR, and the rates were found to be indistinguishable. The parallel pathway predicts that when both Cyt b_{559} and Car are prereduced, the relative amounts of Cyt $b_{559}{}^+$ and Car^+ produced upon illumination at 20 K should depend directly on their relative electron donation rates. The measured similarity in the donation rates thus predicts comparable yields of oxidation for both donors. However, what is observed experimentally is that Cyt b_{559} oxidation occurs almost exclusively, and this argues strongly against the parallel pathway. The lack of Car^+ as a detectable intermediate is attributed to rapid electron transfer from Cyt b_{559} to Car^+. The trapping of Car^+ at low temperature when Cyt b_{559} is preoxidized but its absence when Cyt b_{559} is prereduced is taken as an argument against the simple linear pathway. Overall, the data reported here and previously favor the branched pathway over the linear pathway, while the parallel pathway is thought to be unlikely. Structural considerations provide further arguments in favor of the branched model.

Photosystem II (PSII)[1] is a transmembrane protein complex that catalyzes the oxidation of water to oxygen and the reduction of plastoquinone to plastoquinol. The absorption of a photon by the chlorophyll(s) known as P680 gives rise to a charge separation in the reaction center of PSII. The electron is rapidly transferred through a series of electron acceptors, a pheophytin, and two plastoquinones (Q_A and Q_B) with a non-heme ferrous iron. The oxidized P680 ($P680^+$) is rapidly reduced by the redox-active tyrosine (Tyr_Z). This Tyr_Z is reduced by the Mn cluster, the supposed site for water oxidation (*1*−*3*).

$P680^+$ is the most oxidizing species in PSII, with an estimated E_m of ∼1.1 V. If $P680^+$ is not rapidly reduced, it can cause oxidative damage to PSII (proteins and chromophores). Indeed, the delivery of electrons from Tyr_Z to the highly oxidizing state $P680^+$ can be blocked or retarded under conditions that are physiologically relevant: (1) during normal functioning of the enzyme where the natural equi-

† P.F. was supported by a fellowship from the Swiss National Science Foundation and A.P. by TMR Grant ERBFMBICT983497.

* Corresponding author. Telephone: 33 1 69 08 86 57. Fax: 33 1 69 08 87 17. E-mail: faller@dsvidf.cea.fr.

‡ Section de Bioénergétiques, CEA CNRS URA 2096.

§ Section de Biophysique des Protéines et des Membranes, CEA CNRS URA 2096.

|| Universita di Verona.

[1] Abbreviations: Car, redox-active carotenoid; Chl, chlorophyll; Chl_Z, redox-active chorophyll in PSII; Cyt b_{559}, cytochrome b_{559}; DM, β-dodecyl maltoside; EPR, electron paramagnetic resonance; HEPES, 4-(2-hydroxyethyl)-1-piperazineethanesulfonic acid; MES, 2-(*N*-morpholino)ethanesulfonic acid; P680, photooxidizable chlorophyll in PSII; PSII, photosystem II; Q_A and Q_B, two quinones acting in series as electron acceptors in PSII; Tyr_Z, tyrosine acting as the electron donor to P680; Tyr_D, tyrosine acting as a side path donor to P680.

10.1021/bi0026021 CCC: $20.00
Published on Web 05/04/2001

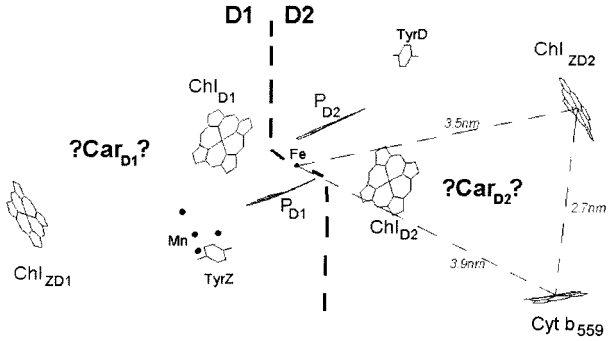

FIGURE 1: Arrangement of the cofactors in PSII based on the crystal structure (*11*) viewed from above the membrane plane (along the C_2 axis). Fe is a non-heme iron ion, Cyt_{559} cytochrome b_{559}, and Mn the manganese cluster, and TyrZ and D are redox-active tyrosine residues where TyrZ is the kinetically competent one. Chl stands for chlorophyll, and the subscripts are just a means of distinguishing them from each other. P also indicates the chlorophylls, but the two of them labeled in this way are the pigments that bear the cation that can be detected by spectroscopy. The two β-carotenes, Car_{D1} and Car_{D1}, were not resolved in ref *11*, and the figure shows their suggested approximate position. D1 and D2 are the polypeptides which bind the cofactors.

libria allow $P680^+$ to be relatively long-lived in a statistical fraction of the centers (see ref *4* for a review; see also ref *5*), (2) in the apoenzyme and during the process whereby the Mn cluster is assembled (e.g., ref *6*), and (3) under stress conditions (reviewed in ref *4*).

If $P680^+$ is not reduced by Tyr_Z, the recombination of the $P680^+Q_A^-$ radical pair [$t_{1/2} \sim 900$ μs (*1*)] is probably dominant under most circumstances. Nevertheless, $P680^+$ seems to be able to obtain electrons from a series of electron donors other than Tyr_Z. Since these "side-path" donation reactions are thought to compete poorly with the usual forward reactions and with charge recombination at room temperature (*1*, *5*), they have more often been studied at low temperatures where the Tyr_Z donation is blocked and the side-path donors can be accumulated using continuous illumination.

The electron donors functioning at low temperatures in PSII have been studied for many years. Knaff and Arnon in 1969 (*7*) discovered that Cyt b_{559} is able to donate electrons at low temperatures. Visser et al. (*8*) showed that when the Cyt b_{559} is preoxidized, illumination results in the oxidation of chlorophyll, among other species. In this article, we refer to this oxidizable chlorophyll as Chl_Z. Later, Schenck et al. (*9*) identified a carotenoid as a low-yield donor at cryogenic temperatures. In isolated PSII reaction centers (D1, D2, and Cyt b_{559}), which lack Q_A and in which Tyr_Z is not redox-competent, Telfer et al. (*10*) studied irreversible carotenoid oxidation by $P680^+$ after illumination in the presence of electron acceptors at ambient temperature.

Figure 1 shows the arrangement of the cofactors in PSII viewed from above the membrane plane based on the recently determined crystal structure (*11*). The resolution was not high enough to distinguish the carotenoids. The structure showed only a single Cyt b_{559}, which is localized on the D2 side. There are two chlorophylls, which are candidates to be the oxidizable Chl_Z symmetrically arranged; the one on the D1 side is called Chl_{ZD1} while that on the D2 side Chl_{ZD2}. Biochemical analyses suggested the presence of two β-carotenes (*12*), perhaps symmetrically bound to D1 (Car_{D1}) and

Scheme 1

a) The linear pathway (20,21) $Cyt\ b_{559} \rightarrow Chl_z \rightarrow Car \rightarrow P680$

b) The branched pathway (20)

$$Chl_z \rightarrow Car \rightarrow P680$$
$$\uparrow$$
$$Cyt\ b_{559}$$

c) The parallel pathway (18)[2]

$$Chl_z \rightarrow Car \rightarrow P680$$
$$\uparrow$$
$$Cyt\ b_{559}$$

D2 (Car_{D2}), as tentatively depicted in Figure 1. Since it is not clear if electron donation can take place from the Car and Chl components on both sides (D1 and D2) of the reaction center (*13*−*16*), in the introductory section and results section of this article, we refer to the oxidizable β-carotene(s) and chlorophyll Car and Chl_Z, respectively, without specifying their localization in D1 or D2. This question is adressed in the Discussion.

Thomson and Brudvig (*17*) investigated electron donation to $P680^+$ from Chl_Z or Cyt b_{559} under conditions where electron donation from Tyr_Z/Mn was progressively inhibited by lowering the temperature. The result showed that Chl_Z and Cyt b_{559} competed equally well with the Tyr_Z pathway, and thus, the Cyt $b_{559} \rightarrow Chl_Z \rightarrow P680$ pathway was suggested. Hillmann and Schlodder (*18*) studied electron donation from Cyt b_{559}, Chl_Z, and Car in PSII from *Synechococcus* at 77 K. When Cyt b_{559} was preoxidized, illumination at 77 K led to about 0.5 Chl_Z^+ and 0.4 Car^+ molecule per reaction center. The Car^+ formation after a flash was measured with a $t_{1/2}$ of 1.9 ms, which was clearly shorter than the $t_{1/2}$ of 3.4 ms for the charge recombination of the $P680^+Q_A^-$ pair. This complex behavior was explained by the $Chl_Z \leftrightarrow Car \rightarrow P680^+$ pathway. An equilibrium between Chl_Z and Car and a comparatively slow donation to $P680^+$ were introduced to explain the near 1:1 accumulation after illumination. Moreover, quantum yields of 8% Cyt b_{559}(ox)/Q_A^- and 5% Car^+/Q_A^- formation per flash were measured. This suggests a faster donation rate to $P680^+$ for Cyt b_{559} than for Car. Thus, a pathway where Cyt b_{559} donates directly to P680 was proposed (the "parallel pathway", Scheme 1c).

Recently, prompted in part by indications of differential temperature dependence for electron donation from carotenoid and chlorophyll reported by Noguchi et al. (*19*), Hanley et al. (*20*) demonstrated that a carotenoid is oxidized in close to stoichiometric amounts by illumination at 20 K in Mn-depleted PSII with preoxidized Cyt b_{559}. In contrast, at higher temperatures (120−200 K), predominantly Chl_Z oxidation is observed. Moreover, after illumination at 20 K, when the carotenoid radical is formed, increasing the temperature to 120 K led to a replacement of the carotenoid with the Chl_Z radical in the dark. This suggested that the carotenoid functions as an electron carrier between Chl_Z and P680. Thus, the $Chl_Z \rightarrow Car \rightarrow P680$ electron pathway seems to occur when Cyt b_{559} is preoxidized. It was also shown that in Mn-depleted PSII, reduced Cyt b_{559} donates electrons to $P680^+$ under illumination at $\leq$20 K, i.e., at a temperature where

[2] In light of the finding by Hanley et al. (*20*), who showed the temperature dependence of the Chl_Z to Car^+ electron donation, the equilibrium between Chl_Z to Car, as suggested by Hillmann and Schlodder (*18*), can be explained instead as arising from the incomplete Chl_Z to Car^+ donation at 77 K.

the $Chl_Z \rightarrow$ Car donation is blocked. The Cyt $b_{559} \rightarrow Chl_Z \rightarrow$ Car $\rightarrow$ P680 linear electron pathway was thus disfavored compared to the branched pathway where both Chl and Cyt donate directly to Car (Scheme 1b). Therefore, the branched pathway was favored over the simple linear pathway. At the same time, Vrettos et al. (*21*) confirmed the earlier reports of a substoichiometic oxidation of Car at 77 K and discussed three pathways, including the Cyt $b_{559} \rightarrow Chl_Z \rightarrow$ Car $\rightarrow$ P680 linear pathway. Taken together, three pathways including the $Chl_Z \rightarrow$ Car step have been proposed as shown in Scheme 1.

In our previous work on Mn-depleted PSII (*20*), we favored the branched pathway over the linear pathway. We did not consider the parallel pathway because we were not aware of the important contribution of Hillmann and Schlodder (*18*). In the work presented here, we address the low-temperature electron pathway to $P680^+$ in oxygen-evolving PSII. The experimental observations obtained previously in Mn-depleted PSII (*20*) were obtained again for PSII with an intact Mn cluster. These allow the linear pathway to be disfavored over the branched pathway. Then a series of experiments are reported which address directly the validity of the parallel pathway.

MATERIALS AND METHODS

PSII-enriched membranes were prepared essentially by the method described in ref *22* with the modifications described in ref *23*. Cyt b_{559} oxidation was achieved either by the method used in Thomson and Brudvig (*17*) (essentially a salt-washing step in the presence of 20 mM $CaCl_2$) or by addition of 5 mM $K_3Fe(CN)_6$. The oxygen evolution after the salt-washing step was not less than 85% of that prior to the treatment and exhibited a value of 400−500 μmol of O_2/mg of Chl measured with a Clark-type electrode (0.3 mM PPBQ as the electron acceptor). Thylakoid membranes were prepared according to the first steps in the PSII membrane preparation and were washed twice in 50 mM HEPES (pH 7.0), 0.3 M sucrose, and 15 mM NaCl.

Mn was depleted from PSII by incubating the membranes (1 mg of Chl/mL) at 0 °C for 15 min in room light in the presence of 2 mM freshly made NH_2OH, and then the sample was transferred to complete darkness, the NH_2OH concentration increased to 4 mM, and the sample incubated again for 30 min at 0 °C. The membranes were then pelleted by centrifugation and washed five times in a buffer containing 5 mM $MgCl_2$, 10 mM NaCl, 1 mM EDTA, and 50 mM MES (pH 6.3) by successive resuspension and centrifugation steps to remove NH_2OH. The final pellet was suspended in 15 mM NaCl, 0.3 M sucrose, and 50 mM MES (pH 6.5). All the washing steps described above were performed in total darkness.

Samples for absorption spectroscopy were prepared according to the method of Hanley et al. (*20*). PSII membranes were solubilized for 30 min with 0.5% *n*-dodecyl β-D-maltoside (DM) at 0 °C and centrifuged to remove unsolubilized material using a benchtop centrifuge. The supernatant was mixed with $K_3Fe(CN)_6$ (to 5 mM) and glycerol (to 60% v/v). Oxygen evolution measurements under saturating light of the solubilized PSII showed an activity of >80% compared to that of the unsolubilized membranes. The samples for time-resolved absorption spectroscopy at low temperatures were prepared with intact or Mn-depleted PSII. For both PSII preparations, the time-resolved absorption spectra were identical for solubilized and unsolubilized material. Addition of $K_3Fe(CN)_6$ (5 mM) was performed immediately before mixing with glycerol (to 60% v/v), whereas addition of ascorbate (1 mM) was done 10 min before mixing with glycerol.

Absorption spectra at low temperatures were collected in an SMC-TBT flow cryostat (Air Liquide, Sassanage, France) cooled with liquid helium, using a Varian Cary E5 double-beam scanning spectrophotometer. Illumination with white light was carried out in the cryostat using a Flexilux fiber optic illuminator. The measuring beam was swept over the spectrum from longer (1150 nm) to shorter wavelengths (750 nm) to minimize possible actinic effects of the measuring beam.

X-Band EPR spectra were recorded with a Bruker ER 300 or 200 spectrometer in an Oxford Instruments cryostat cooled with liquid helium. Illumination at 5 K was carried out in the cavity using an 800 W tungsten lamp filtered through 5 cm water and three infrared cutoff filters. Warming of EPR samples to 198 K and incubation at this temperature were conducted in a solid CO_2/ethanol bath.

To measure the *g* value and line width for the radical signals, the signal of $Tyr_D^\bullet$ before generation of the radical by illumination was subtracted. The number of spins per PSII for Chl^+ and Car^+ was assessed relative to the $Tyr_D^\bullet$ signal obtained in the same sample after illumination for 2 min at 273 K in the presence of 5 mM $K_3Fe(CN)_6$ followed by dark adaptation for 2 min.

For time-resolved absorption at cryogenic temperatures, the measuring light was provided by a 200 W tungsten−halogen lamp and the wavelength was selected with interference filters with a 35 nm bandwidth (fwhm) placed before and after the cuvette (1 cm path length) containing the sample. Absorption changes were detected with a germanium photodiode with a 5 mm diameter [type J16-85P-R05M-HS from EG&G Judson (Montgomeryville, PA)]. Excitation was provided by flashes (6 ns duration, 694.3 nm wavelength) from a ruby laser (Quantel) which saturated the photochemistry of PSII under our experimental conditions.

RESULTS

To distinguish among the different models of the electron pathway (Scheme 1) at low temperatures, first the basic $Chl_Z \rightarrow$ Car $\rightarrow P680^+$ sequence as suggested from the earlier work in Mn-depleted PSII (*20*) was demonstrated for the oxygen-evolving PSII with preoxidized Cyt b_{559}.

$Chl_Z \rightarrow$ Car $\rightarrow$ P680 in Oxygen-Evolving PSII with Preoxidized Cyt b_{559}. Panel A in Figure 2 shows the absorption difference spectra of Mn-containing PSII in which Cyt b_{559} was preoxidized. The sample was illuminated for 30 s at 5 K, then warmed to 120 K in darkness, incubated for 30 min, and recooled to 20 K. The upper trace shows the difference spectrum of the intact PSII membranes before and after illumination at 5 K. The illumination induced a large band at ~990 nm with a shoulder at ~860 nm. The band at 990 nm is similar to those arising in carotenoid cations in vitro (*24*, *25*) which has been reported previously for different PSII preparations (*9*, *18*−*21*, *27*). Accordingly, the signal is attributed to a carotenoid cation radical. The

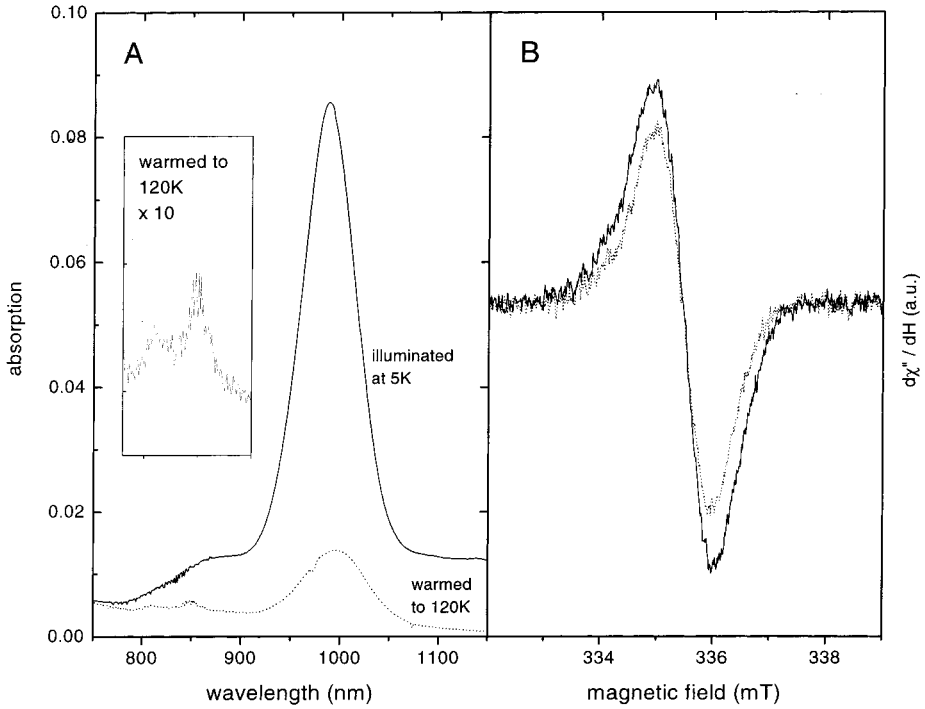

FIGURE 2: (A) Absorption difference spectra of oxygen-evolving PSII, where Cyt b_{559} is in the low-potential form and thus oxidized, due to the salt treatment (see Materials and Methods). Absorption difference spectra generated by illumination at 5 K (upper spectrum) and after warming the same sample to 120 K for 30 min in the dark and then returning the temperature to 20 K (lower spectrum). The inset shows the Chl cation radical absorption region of the spectrum amplified by 10. The chlorophyll concentration was 1 mg/mL and the path length 1 mm, in 50 mM MES (pH 6.5), 15 mM NaCl, 0.3 M sucrose, and 60% glycerol. (B) EPR difference spectra corresponding to panel A. The solid line represents the spectrum induced upon illumination at 5 K (illuminated minus dark spectrum). The dotted line is the difference of the spectrum taken after illumination at 5 K, transfer to an EtOH/dry ice bath (198 K), incubation for 20 min, and returning to 15 K minus the dark spectrum (before illumination). Instrument conditions were as follows: measuring temperature, 15 K; microwave frequency, 9.4 GHz; modulation amplitude, 0.2 mT; power, 0.5 μW; and modulation frequency, 100 kHz.

lower trace exhibits the difference spectrum obtained from the same sample after warming to 120 K and recooling to 20 K minus the spectrum taken before illumination. This treatment results in a decrease in the intensity of the 990 nm band (to less than 15% of that before warming) and the appearance of a band at ~850 nm with a shoulder at ~820 nm. These bands are attributed to Chl_Z^+ on the basis of the comparison with in vitro spectra (*28*) and in accordance with earlier investigations on the Mn-depleted PSII membranes (*16*, *20*, *21*).

The corresponding EPR spectra were also measured and are shown in panel B of Figure 2. After illumination at 5 K, the EPR signal induced is typical for an organic radical with a g value of 2.0025 ± 0.0001 and a line width of 10.5 ± 1 G. The uncertainties in the width and g value derive from sample to sample variation because of the subtraction of the signal from $Tyr_D^\bullet$ [$Tyr_D^\bullet$ was reduced by the NH_2OH used for Mn depletion (*20*)]. By comparison to the fully oxidized $Tyr_D^\bullet$, the signal represents 0.8 spin per reaction center (for details, see Materials and Methods). After warming to 198 K and recooling in the dark (see ref *20*), a similar signal is detected with similar parameters (dotted line in Figure 2B). The intensity reflects 0.65 spin per reaction center. Warming to 198 K in the EPR experiment was carried out to allow a more complete conversion from Car^+ to Chl^+. The lower temperature used in the optical measurements was chosen to avoid the phase transition of the sample containing 60% glycerol. The amount of spins obtained from the EPR measurements approximately correspond to the absorption measurements. When the extinction coefficients reported in the literature for Car^+ are considered (i.e., 130 000, 160 000, and 218 000 from refs *24*, *30*, and *25* respectively), illumination at 5 K results in 1.2, 1.0, or 0.7 equiv per reaction center. After incubation at higher temperatures, 0.09−0.16 equiv of Car^+ and 0.55 equiv of Chl^+ are estimated by applying an extinction coefficient of 6000 (*28*) for Chl^+.

Illumination at 5 K results in the generation of Car^+ in near stoichiometric amounts. The shoulder at 860 nm induced after illumination at 5 K in intact PSII was not reported in ref *20*. However, our more recent studies show it can often be present in Mn-depleted PSII as well. Its origin and the reason for its presence or absence are not clear, but when present, the shoulder always arises and disappears in parallel with the 990 nm band of the Car^+. This indicates that the shoulder at 860 nm is related to Car^+ and not to Chl_Z^+. Due to the shoulder at 860 nm, the presence of Chl_Z^+ formed at 5 K cannot be directly excluded; however, the EPR measurement shows less than one radical per PSII, so given the estimate of the Car^+ from its absorption (at least 0.7 per reaction center), the contribution from Chl^+ must be small under these conditions. When heating to higher temperatures is carried out (120−200 K), Chl_Z^+ is predominantly formed as seen in the absorption spectrum. The quantification indicates the EPR and absorption measurements correspond well with similar amounts of the radicals (0.65 per reaction center) being estimated. The absorption spectra allow the assignment to ~0.55 Chl_Z^+ and 0.09−0.16 Car^+ molecule. Although less clear than the earlier work, these measurements

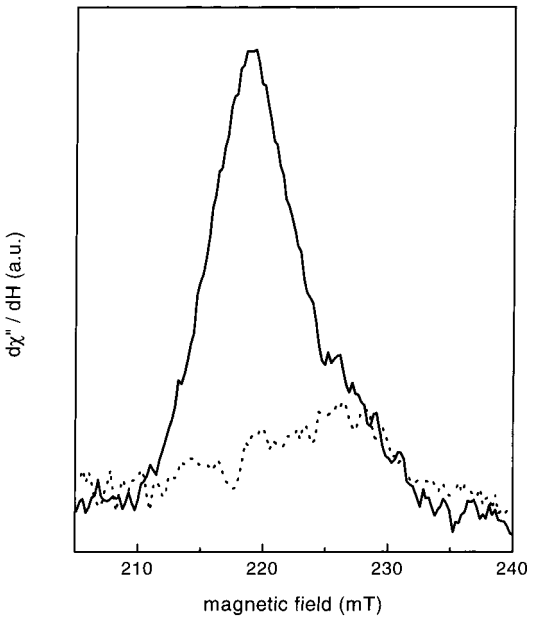

FIGURE 3: EPR spectra of the g_Z of oxidized Cyt b_{559} heme. Untreated oxygen-evolving PSII (containing mostly high-potential Cyt b_{559}) was reduced with ascorbate and dark-adapted (dashed line) and then illuminated (10 min) at 20 K (solid line). The EPR instrument settings were as follows: power, 10 dB; modulation amplitude, 2.5 mT; and temperature, 15 K.

taken in PSII with an intact Mn cluster are very similar to those reported in Mn-depleted PSII (*20*). The data are similarly interpreted as reflecting a sequential electron transfer taking place with Car being the electron donor to $P680^+$ and Chl_Z being the electron donor to Car^+ ($Chl_Z \rightarrow Car \rightarrow P680$), and where the $Chl_Z \rightarrow Car$ step has an energy barrier which can be only overcome at temperatures of >20 K.

Cyt b_{559} Donation to $P680^+$ in Oxygen-Evolving PSII. Hanley et al. (*20*) showed that in the Mn-depleted PSII, prereduced Cyt b_{559} is oxidized upon illumination at 20 K, while at the same temperarure, the $Chl_Z \rightarrow Car$ step was found to be blocked in samples with preoxidized Cyt b_{559}. The linear electron pathway (Cyt $b_{559} \rightarrow Chl_Z \rightarrow Car \rightarrow P680$) includes the $Chl_Z \rightarrow Car$ step, and therefore, it was considered to be the less likely of the two options that were proposed to explain the data (i.e., the branched and linear pathway) (*20*).

Here we have carried out the same experiment in oxygen-evolving PSII. This is of interest because the oxygen-evolving PSII contains predominantly Cyt b_{559} in the high-potential form (midpoint potential of 350 mV) (*31*), while the Cyt b_{559} in Mn-depleted PSII is predominantly in the low-potential form (midpoint potential of 0−80 mV) (*31*). Thus, it is conceivable that the different Cyt b_{559} forms influence the electron pathways.

Figure 3 shows the g_Z feature of EPR signals arising from the $S = {}^1/_2$ ferric heme of oxidized Cyt b_{559}. Prior to illumination, the majority (80−90%) of the Cyt b_{559} was reduced by incubation in darkness with sodium ascorbate. The broken line shows the g_Z peak from the remaining fraction (10−20%) of oxidized Cyt b_{559} heme prior to illumination. The g_Z value of ≈2.95 shows that this fraction is Cyt b_{559} in the low-potential form (*32*; for a review, see ref *33*). The EPR spectra show that Cyt b_{559} is oxidized upon illumination at 20 K (solid line). The intensity was similar to that of samples where Cyt b_{559} was oxidized chemically by K_2IrCl_6, suggesting that complete oxidation was achieved by illumination at 20 K (not shown). Similar results were obtained when illumination was carried out at 5 K. After illumination, a small radical EPR signal was detected which was attributed to Car^+ generated in the small fraction of centers lacking reduced Cyt b_{559} prior to illumination (see below).

From these two experiments, it seems clear that the electron transfer events occurring at low temperatures in intact PSII are similar to those occurring in Mn-depleted PSII. In both cases, the data argue against the simple linear pathway.

Attempt To Detect the Transient Car^+ Signal. In the linear model (Cyt $b_{559} \rightarrow Chl_Z \rightarrow Car \rightarrow P680$) and the carotenoid branching model, Car acts as an intermediate donor between Cyt b_{559} and P680. This is not the case in the parallel pathway in which Cyt b_{559} donates directly to $P680^+$. We have thus attempted to detect a light-induced Car^+ intermediate using time-resolved absorption spectroscopy at 970 nm with Cyt b_{559} being either preoxidized or prereduced. The experiments were carried out at 20 K to exclude complications due to electron donation from Chl_Z, which is virtually absent at this temperature. In Figure 4, the time courses of flash-induced absorption changes are shown. In the presence of 5 mM $K_3[Fe(CN)_6]$ when Cyt b_{559} is oxidized, Car^+ is formed with a rise time ($t_{1/2}$) of ∼2 ms with an amplitude corresponding to a small yield (∼10% per flash; see below). On a longer time scale (Figure 4B), the absorption decays very slowly. This decay was too slow to be characterized completely with the setup used in this study. Nevertheless, attempts to fit the decay yielded a $t_{1/2}$ of several seconds and an amplitude of ∼30% of the maximal signal.

In the presence of 1 mM ascorbate, which reduces Cyt b_{559} in the majority of centers, identical kinetics were observed but with a lower intensity (∼30%), and this we ascribe to a residual fraction of centers in which unreduced Cyt b_{559} is still present (see below). No additional features were detected. Thus, we were unable to detect a transient Car^+ signal under the conditions that were tested. Note that under the condition used Q_A is not reduced and thus charge separation is still possible (see below and Figure 5 inset).

Relative Donation Rates of Cyt b_{559} and Car. The electron donation rates of Cyt b_{559} and Car were investigated using time-resolved absorption and EPR spectroscopy. Since at 20 K the dominating event is the charge recombination between $P680^+$ and Q_A^- ($t_{1/2} \sim 2$ ms) (see ref *1*), the apparent oxidation kinetics of Car and Cyt b_{559} are dominated by the charge recombination reaction. This results in measured oxidation kinetics of ∼2 ms for Car (Figure 4) and Cyt b_{559} oxidation (*18*; see also refs *8* and *34*). However, the intrinsic rates can be deduced from the quantum yield of Cyt b_{559} and Car donation assuming that the electron donation competes with the charge recombination ($P680^+Q_A^-$). The latter has been reported to be independent of the presence of $K_3[Fe(CN)_6]$ (*34*), and this is also the case in our measurements (see the inset of Figure 5). Therefore, the quantum yield of the Car and Cyt b_{559} donation can be compared directly.

These quantum yields were measured indirectly by estimating the number of centers that are able to form the

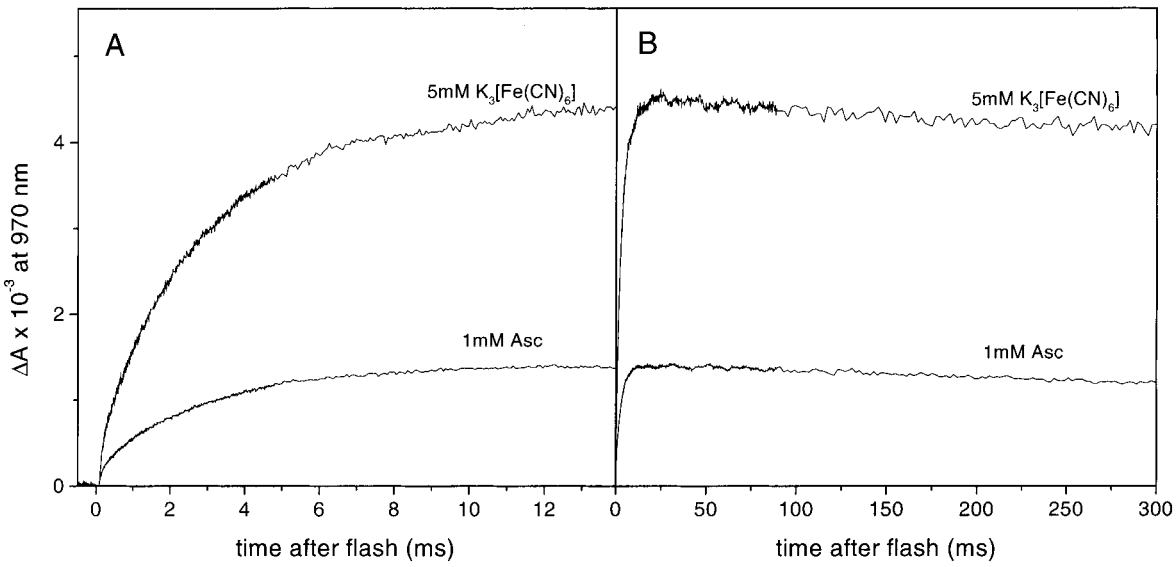

FIGURE 4: Kinetic traces of laser flash-induced absorption changes at 970 nm of untreated oxygen-evolving PSII (containing mostly high-potential Cyt b_{559}) at 20 K under reducing (1 mM ascorbate) and oxidizing {5 mM $K_3[Fe(CN)_6]$} conditions. Panels A and B show the same experiment but on different time scales. The chlorophyll concentration was 0.09 mg/mL and the path length 10 mm, in 50 mM MES (pH 6.5), 15 mM NaCl, 0.3 M sucrose, and 60% glycerol.

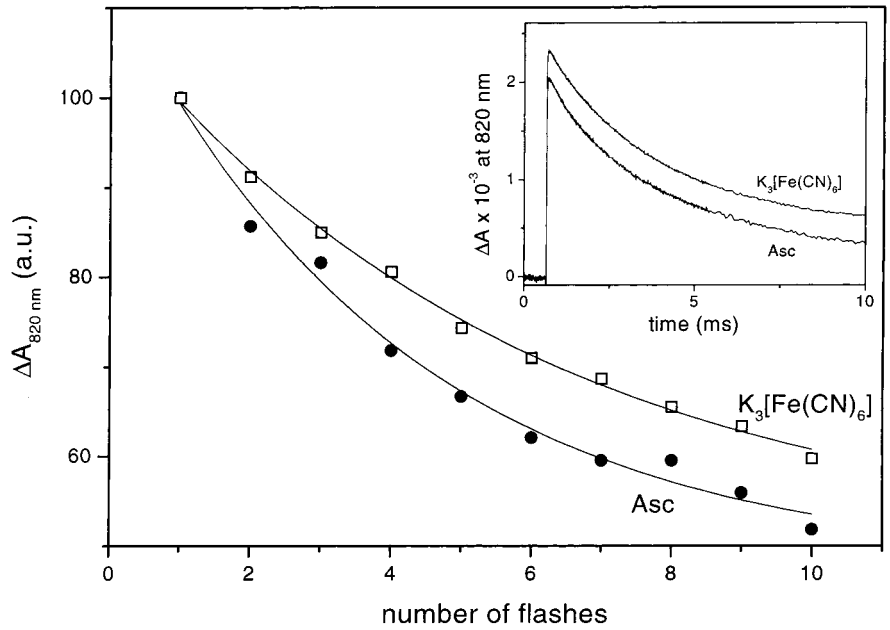

FIGURE 5: Decay of the amplitude of the transient absorption at 820 nm for the first 10 flashes in intact PSII at 20 K (containing mostly high-potential Cyt b_{559}): (●) PSII treated with 5 mM $K_3[Fe(CN)_6]$ and (□) PSII treated with 1 mM ascorbate. Both are fitted with a monoexponential decay curve, shown as a solid line. The inset shows the time-resolved absorption of the first flash in the presence of 5 mM $K_3[Fe(CN)_6]$ and in the presence of 1 mM ascorbate. The chlorophyll concentration was 0.09 mg/mL and the path length 10 mm.

$P680^+Q_A^-$ radical pair (monitoring $P680^+$ at 820 nm) after a series of saturating flashes. In this method, which was used at 77 K by Hillmann and Schlodder (*18*), the decrease in the level of $P680^+$ induced by each flash is attributed to the stable charge separation state $Car^+Q_A^-$ or Cyt $b_{559}(ox)Q_A^-$. A monoexponetial decay was fitted over the first 10 flashes (Figure 5). The amplitudes of the fit in the presence of either $K_3[Fe(CN)_6]$ or ascorbate are very similar, i.e., 50%. The quantum yields extracted from this fit were ~8.3% in the presence of $K_3[Fe(CN)_6]$ and ~11.7% in the presence of ascorbate. When it is considered that under reducing conditions only ~70% Cyt b_{559} is reduced, a corrected quantum yield for the formation of Cyt $b_{559}(ox)Q_A^-$ pair of ~13.2% is obtained. The values are higher than ~5% in the presence of $K_3[Fe(CN)_6]$ and ~8% in the presence of ascorbate reported for *Synechococcus elongatus* at 77 K, but the ratios of values (5%/8% and 8%/13%) are similar (*18*).

From these quantum yields, the donation rates of Cyt b_{559} and Car at 20 K can be calculated. Both donors are in competition with the $P680^+Q_A^-$ recombination with a $t_{1/2}$ of ~2 ms. A yield of 8% for the $Car^+Q_A^-$ pair and a yield of 13% for the Cyt $b_{559}(ox)Q_A^-$ pair give $t_{1/2}$ values of ~25 and ~15 ms, respectively. As described below, we consider that the rate for electron donation may be underestimated by this method since the apparent quantum yield may be underestimated due to recombination of the $Car^+Q_A^-$ pair occurring in some centers.

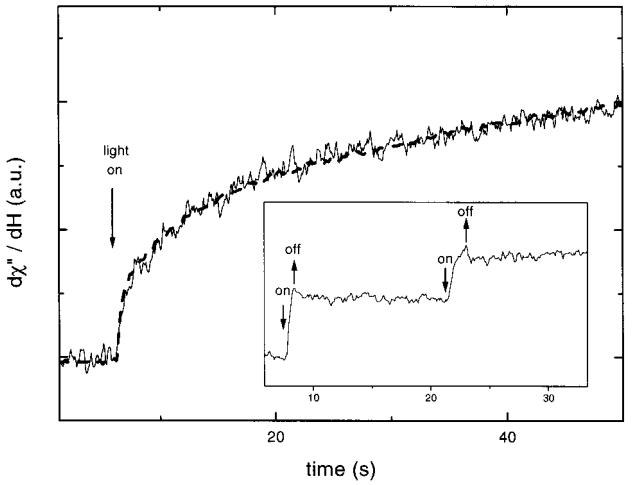

FIGURE 6: Time-resolved EPR measurements at 20 K of intact PSII (containing mostly high-potential Cyt b_{559}). Arrows pointing downward indicate light on and arrows pointing upward light off. The solid line and the inset depict data for PSII with prereduced Cyt b_{559}. The oxidation of Cyt b_{559} was followed at 220 mT. EPR conditions were as follows: microwave power, 25 mW; frequency, 9.4 GHz; and modulation amplitude, 2.5 mT. The dotted line depicts data for PSII with preoxidized Cyt b_{559}. The oxidation of Car upon illumination was followed at 335.5 mT. EPR conditions were as follows: microwave power, 10 μW; frequency, 9.4 GHz; and modulation amplitude, 2.5 mT.

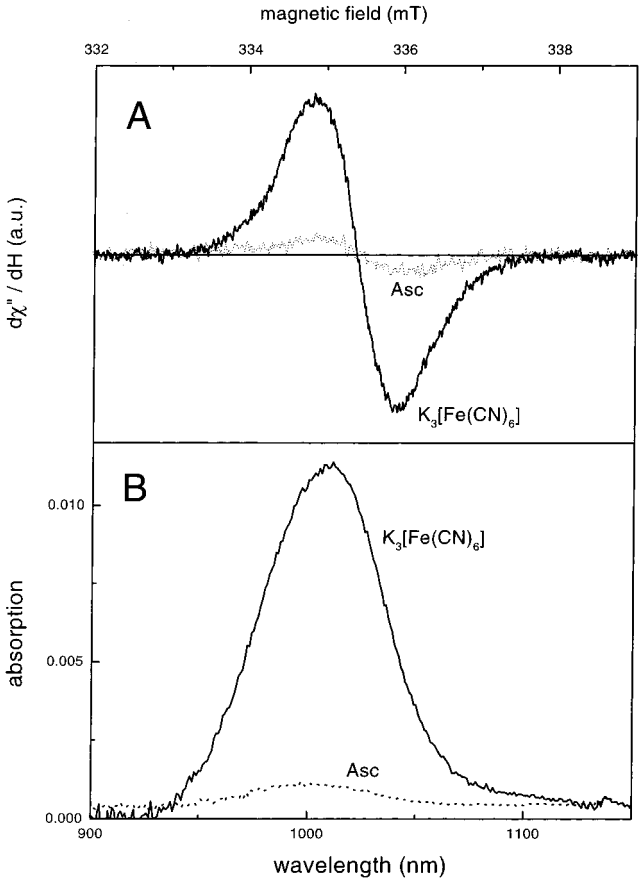

FIGURE 7: (A) Light minus dark difference EPR spectra of PSII (containing mostly high-potential Cyt b_{559}). Car^+ signal induced (light minus dark) by illumination for 10 min at 20 K in the presence of 3 mM ascorbate (dotted line) and 5 mM $K_3[Fe(CN)_6]$ (solid line). EPR conditions were as follows: microwave power, 0.5 μW; frequency, 9.4 GHz; and modulation amplitude, 0.2 mT. There were four accumulations. (B) Absorption difference spectra of chloroplasts (containing mostly high-potential Cyt b_{559}) at 20 K induced by a 30 min illumination at 5 K (illuminated minus dark). Either 5 mM $K_3[Fe(CN)_6]$ or 3 mM ascorbate was added. The chlorophyll concentration was $\approx$0.03 mg/mL and the path length 10 mm, in 50 mM HEPES (pH 7), 15 mM NaCl, 0.3 M sucrose, and 60% glycerol.

Since the oxidation rate of Car or Cyt b_{559} is determined by competition between the rate of donation to $P680^+$ and the rate of recombination of the $P680^+Q_A^-$ pair, the measurement of the oxidation rates of Car or Cyt b_{559} upon the onset of continuous illumination should represent valid relative rates. Since the recombination rate of the $P680^+Q_A^-$ pair is the same under reducing and oxidizing conditions, the oxidation rates can be compared directly. For this purpose, the oxidations of Cyt b_{559} and Car under continuous illumination at 20 K were directly followed by EPR. Figure 6 shows the time course of Cyt and Car oxidation under continuous illumination. The kinetics match very well. The oxidation kinetics of Cyt b_{559} and Car were dependent on PSII concentrations, light intensity, and transparency (the presence of glycerol), but the match of the Cyt b_{559} and Car oxidation kinetics was unaffected by the different conditions.

$P680^+$ exhibits an EPR signal at about the same magnetic field as Car^+ and can therefore contribute to the result. Conditions were chosen to minimize the contribution of $P680^+$. It is known that $P680^+$ is unstable (approximate lifetime of 2 ms at the helium temperature), decaying rapidly by charge recombination with Q_A^- when the light is switched off (e.g., refs *8* and *35*). The inset of Figure 6 shows that after the light is switched off the signal remains stable, suggesting that the signal is due to Car^+ with a negligible $P680^+$ contribution. The light intensity that is used is assumed to be too weak to accumulate more than trace amounts of $P680^+$.

Yield of Car Oxidation under Reducing Conditions. The results reported in the previous section suggest similar electron donation rates for Car and Cyt b_{559}. Therefore, under reducing conditions (i.e., the addition of ascorbate) where both Car and Cyt b_{559} are capable of donating electrons to $P680^+$, the parallel electron donation pathway (Cyt $b_{559} \rightarrow$ P680 $\leftarrow$ Car) is expected to result in the oxidation of approximately equal quantities of each of the terminal donors. On the other hand, for the pathways in which Car is a high-potential intermediate [E_m of in vitro Car $\approx$ 1 V (*36*)] functioning as an electron carrier between Cyt b_{559} and P680, illumination should result in the stable oxidation of only the Cyt b_{559}, it being the lowest-potential donor [$E_m = 0-360$ mV (*31*)].

In Figure 4, the yield of light-induced Car oxidation under reducing conditions is $\sim$30%, but this may be attributable to the residual centers where Cyt b_{559} is still oxidized prior to illumination. Efforts were thus made to obtain samples with a higher proportion of reduced Cyt b_{559}. It is known that high concentrations of glycerol favor the oxidation of Cyt b_{559} (*8*, *37*). In thylakoid membranes, Cyt b_{559} was reported to be less susceptible to oxidation induced by glycerol (*9*). Therefore, studies on thylakoids were conducted, and the results of these are shown in Figure 7B. Under reducing conditions (1 mM ascorbate) in this material, only $\sim$6% of Car^+ is induced by illumination compared to that formed in samples under oxidizing conditions {5 mM $K_3[Fe(CN)_6]$}.

To circumvent the oxidation of Cyt b_{559} by glycerol, analogous measurements were taken by EPR in the absence of glycerol for PSII particles (Figure 7A). Under reducing conditions (3 mM ascorbate), 15% of the Car^+ is formed after illumination at 20 K when compared to the amount of Car^+ formed in the presence of $K_3[Fe(CN)_6]$.

DISCUSSION

In this work, we have attempted to distinguish between the three-electron transfer pathways involving Cyt b_{559}, Car, and Chl_Z that have been proposed to occur in PSII at low temperatures.

The absorption and EPR measurements suggest that illumination at ≤20 K of oxygen-evolving PSII with preoxidized Cyt b_{559} induces almost stoichiometric amounts of Car^+. After PSII had been warmed to higher temperatures (120−200 K), Car^+ was mostly replaced with Chl_Z^+. This indicates a sequential electron pathway in which Car is the electron donor to $P680^+$ and Chl_Z is the donor to Car^+ ($Chl_Z \rightarrow Car \rightarrow P680$). In addition, it appears that the $Chl_Z \rightarrow Car$ step has an energy barrier which can be overcome only at the higher temperatures. These features are very similar to those reported earlier in the Mn-depleted PSII (*20*). Support for this model also comes from studies using ESEEM (*38*), high-field EPR (*39*), and pulse ENDOR (*40*) also using Mn-depleted PSII, and in the case of ENDOR also Mn-containing PSII (*40*), all of which indicate almost exclusive formation of Car^+ at ≤20 K and Chl^+ formation at 198 K.

Studies with prereduced Cyt b_{559} in PSII with an intact Mn cluster showed that Cyt b_{559} is able to donate electrons to $P680^+$ at ≤20 K. As with the earlier work on Mn-depleted PSII (20), the same conclusion can be drawn; the linear pathway (Cyt $b_{559} \rightarrow Chl_Z \rightarrow Car \rightarrow P680$) is disfavored by this result because in this model Cyt b_{559} oxidation is predicted to involve the $Chl_Z \rightarrow Car$ step, and this step is blocked at this temperature (see above).

However, as already suggested in ref *20*, these data can be reconciled with the linear pathway if oxidized Cyt b_{559} has an (electrostatic) effect on the adjacent Chl_Z, increasing its redox potential, thus making it a less efficient donor and leading to the temperature-dependent electron transfer block of the $Chl_Z \rightarrow Car^+$ step. Since this is an ad hoc assumption, we consider the linear model to be a less straightforward explanation than the other pathways, although it remains a possibility. In the subsequent discussion, we focus on trying to discriminate between the parallel and branched pathways.

For PSII with reduced Cyt b_{559}, the branched model predicts Car^+ as an intermediate between $P680^+$ and Cyt b_{559}. In contrast, the parallel pathway predicts that Cyt b_{559} donates directly to $P680^+$, and thus, no transient Car^+ signal should be detected. Indeed, no transient Car^+ was detected. However, the lack of an intermediate can also be reconciled with the branched pathway if it is assumed that the electron donation of Cyt b_{559} to Car^+ is much faster than the rate of electron donation from Car to $P680^+$. Under such circumstances, the Car^+ that is formed is reduced so rapidly by Cyt b_{559} that Car^+ never builds up to a detectable level. Below, we find in favor of the branched model, and thus, we must adopt this explanation for the absence of a Car^+ intermediate.

Since a direct proof (i.e., the presence of a transient Car^+) of the pathway seems not to be possible, another, indirect attempt to discriminate between the branched and parallel pathways was undertaken. In the branched pathway when Cyt b_{559} and Car are both prereduced, low-temperature illumination should result in the oxidation of only Cyt b_{559}, whereas in the parallel pathway, the ratio of Cyt b_{559}(ox) to Car^+ should depend directly on the donation rates of each of these electron donors (see Scheme 2). Thus, the determination of the rates of donation of Cyt b_{559} and Car to $P680^+$ and the yield of oxidation of each donor under reducing conditions should allow discrimination between the two pathways.

Scheme 2[a]

Branched Pathway:

$$\text{Cyt } b_{559}(\text{red}) \rightarrow \text{Car} \rightarrow \text{P680} \quad \xRightarrow[\text{Illumination}]{} \quad \text{Cyt } b_{559}(\text{ox}) \rightarrow \text{Car} \rightarrow \text{P680}$$

100% 100%

Parallel Pathway:

$$\begin{array}{ccccc} \text{Car} \rightarrow \text{P680} & & \text{Car}^+ \rightarrow \text{P680} & & \text{Car} \rightarrow \text{P680} \\ \uparrow & \xRightarrow[\text{Illumination}]{} & \uparrow & + & \uparrow \\ \text{Cyt } b_{559}(\text{red}) & & \text{Cyt } b_{559}(\text{red}) & & \text{Cyt } b_{559}(\text{ox}) \\ 100\% & & X\% & & 100\text{-}X\% \end{array}$$

[a] Chl_Z and Q_A are omitted for clarity, and because Chl_Z donation is blocked at 20 K.

The EPR studies using continuous illumination (Figure 6) suggest approximately similar electron donation rates for Cyt b_{559} and Car to $P680^+$. This is supported by the time-resolved absorption studies (Figure 5) that provide an estimate of the donation rates through a measurement of the quantum yield for stable charge separation. This type of measurement averaged over the first 10 flashes indicates that the electron donation rates of Cyt b_{559} and Car are approximately the same (Figure 5). However, as reported previously (*18*), the quantum yield of Cyt b_{559} oxidation is ~1.6 times larger than for Car. Two factors could contribute to the lower yield of Car oxidation. (1) The slow decay ($t_{1/2}$ of several seconds) of Car^+ attributable to recombination of Car^+ with Q_A^- is expected to lower the quantum yield of stable Car oxidation compared to that of Cyt b_{559}. Hillmann and Schlodder (*18*) reported a recombination of Car^+ with Q_A^- in a fraction of centers. They observed several types of kinetics of charge recombination of Car^+ and Chl_Z^+ with Q_A^-, the fastest one with a $t_{1/2}$ of <10 s. Furthermore, Hanley et al. (*20*) reported a fraction of centers in which $Car^+Q_A^-$ recombination took place in competition with electron donation from Chl_Z. Also relevant to this point is the fact that the driving force for electron donation from Car to $P680^+$ may not be as great as was previously thought (*20*). Indeed, it was pointed out recently that the redox potential of the Car/Car^+ couple in vitro is in fact close to 1 V (*36*). (2) In the branched model, the oxidized Cyt b_{559} might be expected to interact electrostatically with Car, increasing its potential and leading to a slightly slower Car donation to $P680^+$. Overall then, the electron donation rates of Cyt b_{559} and Car are about the same (within a factor of 2). This is in agreement with other studies measuring the quantum yield of the two donors (*18*; see also refs *8* and *34*).

The amount of photoinducible Car^+ in intact PSII in the presence of ascorbate (when Cyt b_{559} is mostly in the high-potential form and therefore reduced in most of the centers and thus is able to donate an electron; see Figure 3) is

reduced to as little as 6% in our experiments, or is even absent as reported by DePaula et al. (*41*). Thus, for the parallel pathway, this would mean that Cyt b_{559} would have to donate approximately 20 times faster than Car, which disagrees with the measured donation rates (maximum of 1.6 times faster). The exclusive oxidation of Cyt b_{559} when it is prereduced is expected in the branched pathway. In this case, the fraction of centers where Car^+ was formed is assigned to incomplete reduction of Cyt b_{559} by ascorbate, due to the presence of the low-potential form in a fraction of centers. This is in agreement with the EPR data (see, for example, Figure 3), where after reduction with ascorbate, a small peak is present at 2250 G ($g_Z \approx 2.95$) arising from the low-potential form of Cyt b_{559} (*32*, *33*). This fits well with reports showing that only 85% of the Cyt b_{559} (the high-potential form) is reduced with ascorbate, and for complete reduction of the low-potential form, stronger reductants such as dithionite or borohydride are needed (*5*). This reflects the fact that the low-potential form of the cytochrome exhibits an E_m ranging from 0 to 80 mV (*31*), and it is thus difficult to oxidize with ascorbate ($E_m = 60$ mV). Overall, we conclude that the branched model fits best to the data presented in this work.

Hillmann and Schlodder (*18*) proposed the parallel pathway because it explains in a simple way why the quantum yield of the Cyt $b_{559}(ox)Q_A^-$ pair is higher than that for the $Car^+Q_A^-$ pair in PSII in which Cyt b_{559} is prereduced and preoxidized, respectively. However, to explain the preference of Cyt b_{559} oxidation under reducing conditions, an electrostatic interaction of Cyt b_{559} with Car^+ or $P680^+$ was invoked; when Cyt b_{559} is reduced, the rate of donation of Car to $P680^+$ is slower, while when Cyt b_{559} is oxidized, the donation rate is faster. From our experiments, the oxidized Cyt b_{559} would have to accelerate the electron donation from Car to $P680^+$ by a factor of 20 to accommodate the parallel pathway. It seems more reasonable to explain the small difference (up to 1.6) by factors other than a separate pathway [i.e., recombination of the $Car^+Q_A^-$ radical pair and a small electrostatic effect of Cyt $b_{559}(ox)$ on the Car as discussed above].

Very recently, the crystal structure of PSII was determined with a resolution of 3.8 Å (*11*) (see Figure 1). Both Chl_Z's (Chl_{ZD1} and Chl_{ZD2}) are distant (>25 Å) from the central chlorophylls (P_{D1} and P_{D2}), on which $P680^+$ is supposed to be located (*11*; see also ref *42*). Cyt b_{559} is also distant from the central chlorophylls (>25 Å) (*11*; see also refs *43* and *44*). These distances are very large for efficient electron transfer in a single step. According to Page et al. (*45*), a 25 Å distance would correspond to a maximal rate of $\sim 1\ s^{-1}$. This is ~2 orders of magnitude slower than the deduced Cyt b_{559} donation rate. Thus, an intermediate, such as the Car, is required. These distance considerations fit well with the experimental evidence for Car functioning as an intermediate for both Chl_Z and Cyt b_{559} oxidation (this work and ref *20*). Moreover, the large separation between Cyt b_{559} and Chl_Z (>25 Å) also argues against direct electron transfer between these components and thus disfavors the linear model. These structural considerations support the branched pathway and put stringent limits on possible arrangements of the carotenoid within the reaction center (see also Figure 1).

In the literature, there has been some debate concerning which side of the reaction center (the D1 side or D2 side) is involved in the side-path electron transfer. Stewart et al. (*16*) investigated *Synechocystis* mutants of the proposed axial ligands of Chl_{ZD1} and Chl_{ZD2} and found that only the mutation on the D1 side affected the resonance Raman signal attributed to Chl_Z^+ and concluded therefore that Chl_Z^+ is located on the D1 side (ref *16*, but see ref *13*). In contrast, Shigemori et al. (*15*) deduced a distance of ~29 Å between TyrD° and Chl_Z^+ in PSII from spinach. This conforms with localization of Chl_Z^+ being on the D2 side (i.e., Chl_{ZD2}). A further argument for the D2 side pathway came from pulsed EPR studies which indicated that Car^+ had a close association with a nearby tryptophan (*38*). Tryptophan residues that were potentially homologous to those making up the carotenoid binding site of the purple bacterial reaction centers were found on the D2 side. Recently, a third option has been proposed; on the basis of the attribution of two features in the Chl_Z^+ absorption spectrum to Chl_{ZD1} and Chl_{ZD2} in PSII from spinach, it was suggested that the electron donation pathway occurs on both sides of the reaction center in spinach PSII (*14*).

The fact that the crystal structure shows a single Cyt b_{559} localized on the D2 side shows that the electron transfer pathway certainly involves D2. The work presented here allows some conclusions to be drawn concerning the possible existence of a symmetrical pathway involving Chl_Z and Car in D1. When Cyt b_{559} is prereduced, illumination at different temperatures leads predominantly to Cyt b_{559} oxidation (>90%) (see above and ref *41*). This indicates that under these conditions Chl_{ZD2} and Car_{D2} are the dominant electron donors, since competing electron donation from the D1 side should be manifest as the formation of Chl_{ZD1} and Car_{D1} radicals. Given that the D2 side is the dominant route when Cyt b_{559} is reduced, then it is also reasonable to assume that this is the case when Cyt b_{559} is oxidized. The suggestion that Chl_Z and Car from both sides of the reaction center in spinach PSII undergo oxidation when Cyt b_{559} is preoxidized (*14*) remains conceivable if the oxidized heme has a marked electrostatic influence on midpoint potentials of the D2 components. The simplest explanation is that a D2 pathway is the predominant operation route in spinach PSII membranes.

ACKNOWLEDGMENT

We thank Dr. P. Mathis for his help with the low-temperature flash-induced absorption measurements, Drs. K. Brettel, A. Boussac, Y. Deligiannakis, J. Hanley, C. Goussias, R. Edge, A. Telfer, D. Kirilovsky, and A. Liszkay-Krieger for helpful discussions, and Dr. P. Setif for providing the data analysis software.

REFERENCES

1. Diner, B. A., and Babcock, G. T. (1996) in *Oxygenic photosynthesis: the light reactions* (Ort, D. R., and Yocum, C. F., Eds.) pp 213−247, Kluwer, Dordrecht, The Netherlands.
2. Britt, R. D. (1996) in *Oxygenic photosynthesis: the light reactions* (Ort, D. R., and Yocum, C. F., Eds.) pp 137−164, Kluwer, Dordrecht, The Netherlands.
3. Debus, R. (1992) *Biochim. Biophys. Acta 1102*, 269−352.
4. Andersson, B., and Barber, J. (1996) in *Photosynthesis and the Environment* (Baker, N. R., Ed.) pp 101−121, Kluwer, Dordrecht, The Netherlands.
5. Buser, C. A., Diner, B. A., and Brudvig, G. W. (1992) *Biochemistry 31*, 11449−11459.

6. Blubaugh, D. J., and Cheniae, G. M. (1990) *Biochemistry 29*, 5109−5118.
7. Knaff, D. B., and Arnon, D. I. (1969), *Proc. Natl. Acad. Sci. U.S.A. 63*, 963−969.
8. Visser, J. W. M., Rijgersberg, C. P., and Gast, P. (1977) *Biochim. Biophys. Acta 460*, 36−46.
9. Schenk, C. C., Diner, B. A., Mathis, P., and Satoh, K. (1982) *Biochim. Biophys. Acta 680*, 216−227.
10. Telfer, A., De La Rivas, J., and Barber, J. (1991) *Biochim. Biophys. Acta 1060*, 106−114.
11. Zouni, A., Witt, H.-T., Kern, J., Fromme, P., Krauss, N., Saenger, W., and Orth, P. (2001) *Nature 409*, 739−743.
12. Nanba, O., and Satoh, K. (1987) *Proc. Natl. Acad. Sci. U.S.A. 84*, 109−112.
13. Ruffle, S., Hutchinson, R., and Sayre, R. T. (1998) in *Photosynthesis: Mechanism and Effects* (Garab, G., Ed.) Vol. II, pp 1013−1016, Kluwer, Dordrecht, The Netherlands.
14. Tracewell, C. A., Cua, A., Stewart, D. H., Bocian, D. F., and Brudvig, G. W. (2001) *Biochemistry 40*, 103−203.
15. Shigemori, K., Hara, H., Kawamori, A., and Akobori, K. (1998) *Biochim. Biophys. Acta 1185*, 257−270.
16. Stewart, D. H., Cua, A., Chisholm, D. A., Diner, B. A., Bocian, D. F., and Brudvig, G. W. (1998) *Biochemistry 37*, 10040−10046.
17. Thompson, L. K., and Brudvig, G. W. (1988) *Biochemistry 27*, 6653−6658.
18. Hillmann, B., and Schlodder, E. (1997) *Biochim. Biophys. Acta 1231*, 76−88.
19. Noguchi, T., Mitsuka, T., and Inoue, Y. (1994) *FEBS Lett. 356*, 179−182.
20. Hanley, J., Deligiannakis, Y., Pascal, A., Faller, P., and Rutherford, A. W. (1999) *Biochemistry 38*, 8189−8185.
21. Vrettos, J. S., Stewart, D. H., de Paula, J. C., and Brudvig, G. W. (1999) *J. Phys. Chem. B 103*, 6403−6406.
22. Berthold, D. A., Babcock, G. T., and Yocum, C. F. (1981) *FEBS Lett. 134*, 231−234.
23. Ford, R. C., and Evans, M. C. W. (1983) *FEBS Lett. 160*, 159−164.
24. Mathis, P., and Vermeglio, A. (1972) *Photochem. Photobiol. 15*, 157−164.
25. Dawe, E. A., and Land, E. J. J. (1975) *J. Chem. Soc., Faraday Trans. 1 71*, 2162−2169.
26. Deleted in proof.
27. Pascal, A., Telfer, A., Barber, J., and Robert, B. (1999) *FEBS Lett. 453*, 11−14.
28. Mathis, P., and Setif, P. (1981) *Isr. J. Chem. 21*, 316−320.
29. Deleted in proof.
30. Moore, T. A., Dust, D., Mathis, P., Mialocq, J.-C., Chachaty, C., Bensasson, R. V., Land, E. J., Doizi, D., Liddell, P. A., Lehman, W. R., Nemethy, G. A., and Moore, A. L. (1984) *Nature 307*, 630−632.
31. Cramer, W. A., and Whitmarsh, J. (1977) *Annu. Rev. Plant Physiol. 28*, 133−177.
32. Berthomieu, C., Boussac, A., Mantele, W., Breton, J., and Nabedryk, E. (1992) *Biochemistry 31*, 11460−11471.
33. Stewart, D. H., and Brudvig, G. W. (1998) *Biochim. Biophys. Acta 1367*, 63−87.
34. Mathis, P., and Vermeglio, A. (1975) *Biochim. Biophys. Acta 369*, 371−381.
35. Ke, B., Inoue, H., Babcock, G. T., Fang, Z.-X., and Dolan, E. (1982) *Biochim. Biophys. Acta 682*, 297−306.
36. Edge, R., Land, E. J., McGarvey, D. J., Burke, M., and Truscott, T. G. (2000) *FEBS Lett. 471*, 125−127.
37. Vermeglio, A., and Mathis, P. (1974) in *Proceedings of the 3rd International Congress on Photosynthesis, Revohot* (Avron, M., Ed.) pp 323−334, Elsevier, Amsterdam.
38. Deligiannakis, Y., Hanley, J., and Rutherford, A. W. (2000) *J. Am. Chem. Soc. 122*, 400−401.
39. Faller, P., Rutherford, A. W., and Un, S. (2000) *J. Phys. Chem. B 104*, 10960−10963.
40. Faller, P., Maly, T., Rutherford, A. W., and MacMillan, F. (2001) *Biochemistry 40*, 320−326.
41. De Paula, J. C., Innes, J. B., and Brudvig, G. W. (1985) *Biochemistry 24*, 8114−8120.
42. Koulougliotis, D., Innes, J. B., and Brudvig, G. W. (1994) *Biochemistry 33*, 11814−11822.
43. Rhee, K.-H. (1998) Ph.D. Thesis, Max Planck Institut fuer Biophysik, Frankfurt, Germany.
44. Kuroiwa, S., Tonaka, M., Kawamori, A., and Akabori, K. (2000) *Biochim. Biophys. Acta 1460*, 330−337.
45. Page, C. C., Moser, C. C., Chen, X., and Dutton, P. L. (1999) *Nature 402*, 47−52.

BI0026021